Remote Sensing of Environment 115 (2011) 1603–1616

Contents lists available at ScienceDirect

Remote Sensing of Environment

journal homepage: www.elsevier.com/locate/rse

Review

Endmember variability in Spectral Mixture Analysis: A review

Ben Somers [a,b,*], Gregory P. Asner [c], Laurent Tits [b], Pol Coppin [b]

[a] Flemish Institute for Technological Research (VITO), Centre for Remote Sensing and Earth Observation Processes (TAP), Boeretang 200, BE-2400 Mol, Belgium
[b] Dept. of Biosystems, M3-BIORES, Katholieke Universiteit Leuven, W. de Croylaan 34, BE-3001 Leuven, Belgium
[c] Dept. of Global Ecology, Carnegie Institution for Science, 260 Panama Street, Stanford, CA 94305, USA

A R T I C L E I N F O

Article history:
Received 12 August 2010
Received in revised form 28 February 2011
Accepted 2 March 2011
Available online 3 April 2011

Keywords:
Mixed pixels
Unmixing
Spectral Mixture Analysis
Mixture modeling
Endmember selection
Endmember variability

A B S T R A C T

The composite nature of remotely sensed spectral information often masks diagnostic spectral features and hampers the detailed identification and mapping of targeted constituents of the earth's surface. Spectral Mixture Analysis (SMA) is a well established and effective technique to address this mixture problem. SMA models a mixed spectrum as a linear or nonlinear combination of its constituent spectral components or spectral endmembers weighted by their subpixel fractional cover. By model inversion SMA provides subpixel endmember fractions. The lack of ability to account for temporal and spatial variability between and among endmembers has been acknowledged as a major shortcoming of conventional SMA approaches using a linear mixture model with fixed endmembers. Over the past decades numerous efforts have been made to circumvent this issue. This review paper summarizes the available methods and results of endmember variability reduction in SMA. Five basic principles to mitigate endmember variability are identified: (i) the use of multiple endmembers for each component in an iterative mixture analysis cycle, (ii) the selection of a subset of stable spectral features, (iii) the spectral weighting of bands, (iv) spectral signal transformations and (v) the use of radiative transfer models in a mixture analysis. We draw attention to the high complementarities between the different techniques and suggest that an integrated approach is necessary to effectively address endmember variability issues in SMA.

Contents

* Corresponding author. Tel.: +32 14336768.
E-mail address: ben.somers@vito.be (B. Somers).

0034-4257/$ – see front matter
doi:10.1016/j.rse.2011.03.003

1. The heterogeneous nature of remotely sensed spectral information

To date the full potential of remotely sensed data analysis for monitoring processes on the earth surface is still not fully employed. One reason is the composite nature of pixels, i.e. discrete elements of the 2D ground space. Since no pixel, however small it might be, represents complete homogeneous characteristics, the measured signal by the sensor always results from the interactions of electromagnetic radiation with multiple constituents within each pixel (Keshava & Mustard, 2002). Numerous remote sensing applications using the visible, near-infrared, short-wave infrared and thermal infrared regions of the electromagnetic radiation, consequently suffer from image interpretation issues as the mixed nature of the spectral information considerably constrains the accuracy of spectral analysis (Adams et al., 1986; Atkinson et al., 1997; Gillespie, 1992; Green et al., 1998; Heinz & Chang, 2001; Keshava & Mustard, 2002; Roberts et al., 1993; Song, 2005).

Over the past decades, a number of image analysis techniques accommodating mixing problems have been proposed (e.g., Atkinson & Tatnall, 1997; Brown et al., 1999; Carpenter et al., 1999; Guilfoyle et al., 2001; Nascimento & Bioucas-Dias, 2005a; Wang, 1990) with Spectral Mixture Analysis (SMA; Adams et al., 1986; Keshava & Mustard, 2002) being one of the most common techniques utilized in many applications. The value of subpixel fraction maps provided by SMA has been demonstrated in climate change research (e.g., Asner & Heidebrecht, 2005; Garcia & Ustin, 2001; Huang et al., 2010; Melendez-Pastor et al., 2010; Xu et al., 2008), terrestrial ecosystem monitoring and management (e.g., Gilabert et al., 2000; Hestir et al., 2008; Painter et al., 2003; Roberts et al., 2004; Roder et al., 2008; Rogan et al., 2002; Wessman et al., 1997), precision agriculture and production monitoring (e.g., Lelong et al., 1998; Liu et al., 2008; Lobell & Asner, 2004; Pacheco & McNairn, 2010; Peddle & Smith, 2005), natural hazard risk assessment (Eckmann et al., 2010; Jia et al., 2006; Katra & Lancaster, 2008; Roberts et al., 2003a), forest inventories and forest health assessments (Asner et al., 2004; Goodwin et al., 2005; Peddle et al., 1999; Soenen et al., 2010), water quality assessment (Mertes et al., 1993; Svab et al., 2005) and fresh water management (Mertes, 2002), geological mapping (Bedini, 2009; Green et al., 1998; Ramsey & Christensen, 1998; Sunshine & Pieters, 1993), mapping of the urban environment (Phinn et al., 2002; Rashed et al., 2003; Small, 2001; Weng et al., 2004; Wu & Murray, 2003) and extraterrestrial mapping surveys (Fischer & Pieters, 1994; Li & Mustard, 2003; Pinet, 1995).

2. Spectral Mixture Modeling

Mixed pixel signals are generally modeled using either a linear (LMM) or nonlinear mixture model (NLMM). A mixture model converts the image DN's to numerical fractions of a few endmembers. Endmembers are spectra that are proxies for materials on the ground (Adams & Gillespie, 2006). The question whether linear or nonlinear processes dominate spectral signatures of mixed pixels is still an unresolved matter. As a rule of thumb, linear mixing is associated to mixtures for which the pixel components appear in spatially segregated patterns. If, however, the components are in intimate association, light typically interacts with more than one component as it is multiply scattered, and the mixing systematics are highly nonlinear (Keshava & Mustard, 2002).

The underlying physical assumption of a LMM is that each incident photon interacts with a single pixel component only. A mixed pixel signal (r) can as such be described as a linear combination of pure spectral signatures of its constituent components (i.e., endmembers), weighted by their subpixel fractional cover (Adams et al., 1986):

$$r = Mf + \varepsilon \tag{1}$$

In Eq. (1) M is a matrix in which each column corresponds to the spectral signal of a specific endmember. f is a column vector $[f_1,\ldots f_m]^T$ denoting the cover fractions occupied by each of the m endmembers in the pixel. ε is the portion of the spectrum that cannot be modeled using these endmembers.

NLMM's account for a nonlinear mixing process, which is a product of multiple scattering between at least two materials in the field of view. Based on the radiosity theory described by Borel and Gerstl (1994), nonlinear mixing effects can be modelled explicitly by including additional endmembers to the LMM, each accounting for a characteristic interaction among ground objects. Using a training data set, the mathematical relationships between input (spectral data) and output data (classes of interest) can also be automatically calculated using advanced computer modeling approaches such as Artificial Neural Networks (Atkinson & Tatnall, 1997; Carpenter et al., 1999; Guilfoyle et al., 2001; Mercier et al., 2005; Weng & Hu, 2008) and decision tree classifiers (i.e., Vegetation Continuous Fields, Morton et al., 2005).

Nonlinear mixing, has been firmly established for mineral soils (e.g., Mustard & Pieters, 1987, 1989; Nash & Conel, 1974; Shipman & Adams, 1987) and water (Mertes et al., 1993) and nonlinear mixing effects have been described and modelled for a variety of vegetation types (e.g., Arai, 2007; Borel & Gerstl, 1994; Chen & Vierling, 2006; Huete, 1986; Ray & Murray, 1996; Roberts, 1991; Roberts et al., 1993; Somers et al., 2009a; Zarco-Tejada et al., 2001).

Nevertheless, the quantitative effects of nonlinear mixing on the accuracy of fractional cover estimates remains poorly understood. The majority of unmixing studies therefore assume linear mixing and apply the LMM as described in Eq. (1). For many problems, the linear model is thought to provide sufficient accuracy to map subpixel abundances in remotely sensed data (Elmore et al., 2000), so much the more because the linear analysis is computationally simpler compared to the often complex NLMM's (Adams & Gillespie, 2006). In these authors's opinion the choice between LMM's or NLMM's depends on the nature of the problem and the scale of the endmembers. Or in other words, it depends on how accurately we need to know the fractions. For a more detailed overview of spectral mixture modeling and the choice between LMM's and NLMM's the reader is advised to read Keshava and Mustard (2002) and Adams and Gillespie (2006).

3. Endmember selection

The key to successful SMA is appropriate endmember selection (Elmore et al., 2000; Tompkins et al., 1997). Selecting endmembers involves identifying both the number and type of endmembers and their corresponding spectral signatures. Optimally, SMA requires that the spectral variability of the image pixels is described with a minimum number of endmembers (Sabol et al., 1992). Too many endmembers, or endmembers that are spectrally similar, lead to endmember fraction images that are physically inaccurate as judged, for example, against field assessments (Song, 2005). Different solutions to select the optimal number and type of endmembers for a specific scene have been proposed. The techniques range from manually testing different sets of endmembers (e.g., Radeloff et al., 1999; Smith et al., 1990; Somers et al., 2010a; Wessman et al., 1997), incorporation of the vegetation–impervious surface–soil (V–I–S) model and linear unmixing in urban areas (e.g., Wu & Murray, 2003; Zhao & Qiu, 2009), to iteratively testing different endmember combinations (Franke et al., 2009; Garcia-Haro et al., 2005; Roberts et al., 1998; Theseira et al., 2002).

The spectral signatures of the endmembers may be derived from spectral libraries built from field or laboratory measurements, obtained using ground based or portable spectro-radiometers (e.g., Asner & Lobell, 2000; Roberts et al., 1998). Yet, endmember reference spectra can also be derived directly from the image data themselves (e.g., Bateson et al., 2000; Plaza et al., 2002) or simulated using radiative transfer models (Collins et al., 2001; Dennison et al., 2006; Eckmann et al., 2008; Painter et al., 2003; Peddle et al., 1999; Sonnetag et al., 2007).

A number of advanced analysis techniques to locate and extract endmembers from image data have been described. Important concepts here include Pixel Purity Index (PPI, Boardman et al., 1995), the virtual endmember concept (Tompkins et al., 1997), and N-FINDR (Winter, 1999). A thorough discussion of these is outside the scope of this review. Theseira et al. (2003), Plaza et al. (2004), Martinez et al. (2006) and Veganzones and Grana (2008), however, have systematically discussed and compared a set of different image endmember extraction techniques. Other significant contributions are from e.g., Craig (1994), Harsayni and Chang (1994), Tu et al. (1997), Bateson et al. (2000), Chang and Heinz (2000), Plaza et al. (2002), Dennison and Roberts (2003a), Nascimento and Bioucas-Dias (2005b),Plaza et al. (2005), Chang and Ji (2006), Rogge et al. (2006), Wang and Chang (2006), Miao and Qi (2007), and Dobigeon et al. (2009).

4. Spectral Mixture Analysis

Once the endmembers and their spectral signatures are known and if the number of endmembers is less than the number of spectral bands, the system of equations in Eq. (1) is over-determined and may uniquely be inverted using techniques to solve for the fractions with minimal additional error in the equations. Commonly used optimization techniques are Singular Value Decomposition (Ball et al., 2004), Gramm-Schmidt Orthogonalization (Adams et al., 1995), Quadratic Programming (Chen et al., 2009; Du, 2004), maximum-likelihood (Settle, 2006) or least squares regression analysis (Barducci & Mecocci, 2005). SMA can be implemented without constrains (e.g., Harsayni & Chang, 1994), but physically meaningful abundance estimates are often obtained by constraining the coefficients in Eq. (1) to sum to unity and to be positive (Adams et al., 1993). The accuracy of SMA is often quantified based on the fit between the modeled and observed mixed spectral signals. Model fit can be assessed by an error metric such as the residual term ε (Rogge et al., 2006) or the Root Mean Square error (RMSE; Roberts et al., 1998). In cases where accurate ground reference data are available, the suitability of the selected endmembers and the quality of the subpixel abundance estimates can be assessed more reliably by checking the discrepancy between the estimated and real endmember fractions (Plaza et al., 2004). The fraction abundance error (Rogge et al., 2006; Somers et al., 2009d) and the coefficient of determination (Elmore et al., 2000; McGwire et al., 2000; Zhang et al., 2004) are widely used discrepancy measures.

5. Endmember variability

Fraction estimate accuracies as provided by SMA are prone to residual spectral error caused by ambient (e.g., inaccurate atmospheric correction; Gong & Zhang, 1999), sensor-specific (e.g., insufficient Signal-to-Noise Ratio; Plaza et al., 2004) and model structure input noise (e.g., nonlinear mixing; Borel & Gerstl, 1994). The most profound source of error in SMA, however, lies in the lack of the ability to account for sufficient temporal and spatial spectral variability (Bateson et al., 2000; Roberts et al., 1992, 1998; Smith et al., 1994). In a conventional Simple SMA (sSMA) approach, image-wide endmember spectra are defined. Based on the available spectral library, a standard (i.e., commonly the mean) spectrum is defined for each of the presented endmembers. The standard endmember spectra are subsequently assigned to each image pixel and subpixel cover fractions are calculated using SMA (e.g., Adams et al., 1993). This approach is straightforward and easy to implement. The technique is considered very useful for fast photo interpretation and field investigations where it is not necessary to know the identities or the proportions of the spectrally dominant materials with high accuracy (Adams & Gillespie, 2006). For many endusers it is easier to interpret an image in terms of the approximate proportions of certain materials on the ground than it is to interpret pixel digital number values that represent radiance, reflectance, or emittance (Adams & Gillespie, 2006).

Nevertheless, many applications require that the proportions of the endmembers are known as accurately as possible (Adams & Gillespie, 2006; Roberts et al., 1998; Somers et al., 2009a). The use of fixed endmember spectra, as in sSMA, implies that variation in endmember spectral signatures, caused by spatial and temporal variability in the condition of scene components and differential illumination conditions, is not accounted for. sSMA can as such provide appropriate accuracies in some relatively homogeneous ecosystems, but because of the spectral complexity of many natural and semi-natural landscapes the use of fixed endmember spectra results in significant fraction estimate errors (Asner & Lobell, 2000; Bateson et al., 2000; Roberts et al., 1998). This problem, illustrated in Figs. 1 and 2 for a citrus orchard, is referred to as the endmember variability problem.

Two types of variability are commonly distinguished: (i) the variability within an endmember class (intra-class variability), and (ii) the similarity among endmember classes (inter-class variability) (Zhang et al., 2006). The accuracy of subpixel fraction estimates linearly decreases with intra-class variability (Barducci & Mecocci, 2005; Settle, 2006). This is logical since the higher the intra-class variability, the higher the likelihood that the actual spectral characteristics of the endmembers in a specific pixel (i.e. one of the black signatures in Fig. 1) deviates from the pre-defined standardized and fixed endmembers used in the sSMA (i.e., the red signatures in Fig. 1). In some environments or for some applications, similarity among reflectance spectra of the different endmembers of interest (e.g., crops and weeds in agricultural fields, Somers et al., 2009c; spectral similarity among minerals, Debba et al., 2006) provides an additional difficulty to obtain accurate classification results (Okin et al., 2001). Similarity between endmembers results in a high correlation between the endmember spectra (R), which in turn leads to an unstable inverse matrix and a dramatic drop in estimation accuracy (Gong & Zhang, 1999).

Over the past decades, numerous solutions to account for endmember variability have been provided and their number is still rising (Somers et al., 2010a, 2010b). Because of the abundant and diverse approaches, researchers often fail to fully acknowledge and integrate previous contributions, with the risk of duplicating and renaming techniques. This evolution requires a comprehensive and structured overview of the available knowledge, which we aim to provide here. In the subsequent sections, the modalities of the most commonly used solutions to address endmember variability in SMA are described in detail. It is hypothesized that all of the available techniques are founded on five basic principles which should be integrated to allow a proper tackling of endmember variability in SMA.

6. How to address endmember variability?

This section gives a comprehensive overview of techniques to reduce the errors in SMA related to endmember variability. Five different conceptual approaches or basic principles are presented: iterative mixture analysis cycles, spectral feature selection, spectral weighting, spectral transformations and spectral modeling.

6.1. *Iterative mixture analysis cycles*

One of the first attempts to address endmember variability was made by Roberts et al. (1998). These authors introduced the use of iterative mixture analysis cycles. In their Multiple Endmember Spectral Mixture Analysis (MESMA) technique, endmembers are

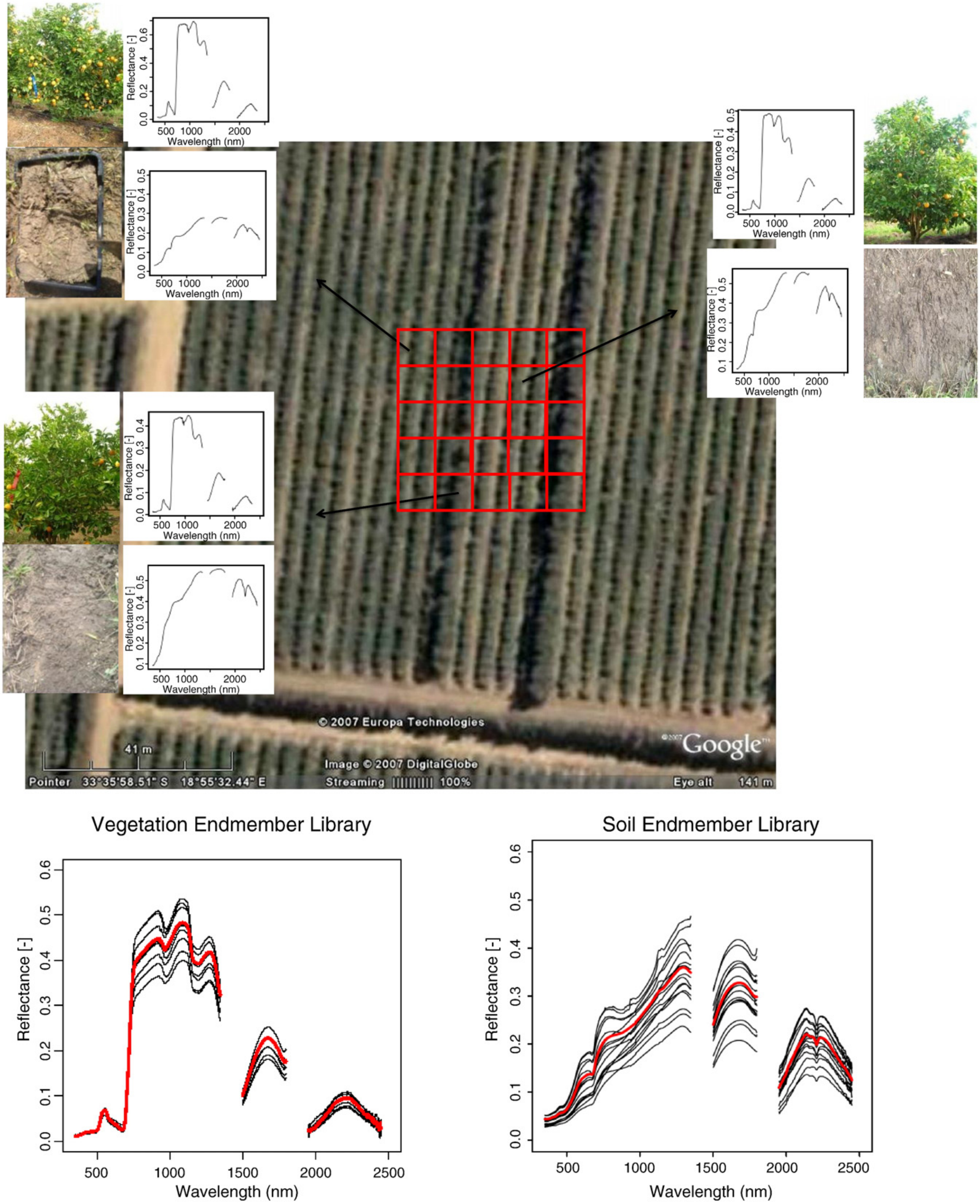

Fig. 1. Illustration of the spatial variability in endmember spectra collected in a citrus orchard plot near Wellington, South Africa (33°35 00 S; 18°55 30 E). Reflectance measurements were acquired using a full-range (350–2500 nm) spectroradiometer with a 25° foreoptic (Analytic Spectral Devices, Boulder, CO) and reflectance was calibrated using a white spectralon panel (Labsphere Inc., North Sutton, NH). Soil reflectance measurements were taken from nadir at 1 m above the soil surface while tree canopy spectra were measured from nadir at 2 m above the tree top using a cherry picker (Somers et al., 2009b). Measurements were performed within one hour of local solar noon. The conditions and consequently the spectral features of each component changes from pixel to pixel. In conventional simple SMA approaches predefined and fixed standard endmember spectra (red solid lines in bottom graphs) are used to decompose the spectral signals of each pixel. The endmember variability from pixel to pixel (black solid lines in bottom graphs) is hence not taken in to account. This drawback of conventional SMA approaches is known as the endmember variability problem.

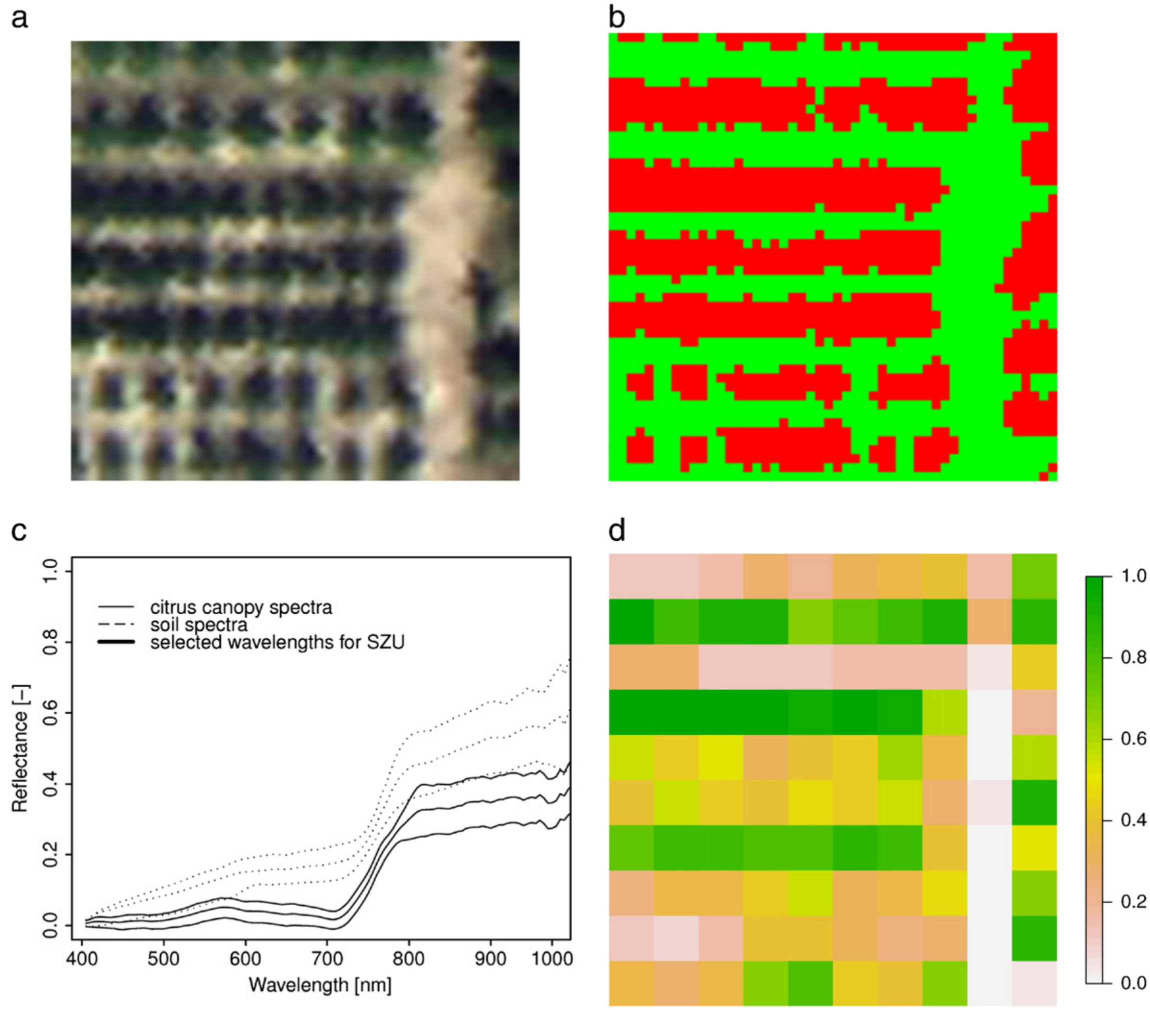

Fig. 2. (a) RGB representation of a spatial subset of an Airborne Imaging Spectrometer for Applications (AISA) Eagle sensor image (Galileo Group Inc., Melbourne, FL, USA), acquired in November 2006 and covering a citrus orchard area in the surroundings of Lake Alfred, Florida, USA (28.13° N, 81.72° W). The AISA sensor is equipped with 127 spectral bands that cover the 400 to 1000 nm spectral range, with an average spectral resolution of ~7 nm. Shuttle Radar Topography mission (SRTM) elevation data were used for geo-rectification. The Ground Instantaneous Field of View is 0.85 m. Radiance data (uW/cm²/str/nm) were converted to relative reflectance data using the Empirical Line technique (Farrand et al., 1994); (b) classified image obtained after an unsupervised k-means classification; (c) corresponding spatial variability in bare soil and citrus canopy spectral properties observed throughout the orchard, illustrating the endmember variability problem; Because accurate ground reference information was lacking, the AISA hypercube was convoluted up to a spatial resolution of 4.25 by 4.25 m pixels (using a 5 by 5 moving average pixel window). Based on the classified image, the relative sub-pixel cover distribution was calculated for each 4.25 m by 4.25 m pixel window. Results for the citrus canopy endmember is shown in (d). The convolved images were used to illustrate the effects of different endmember variability reduction techniques described in Section 6. The canopy cover map in (d) is used as a reference to validate the output of the different SMA techniques. Results are shown in Fig. 3.

allowed to vary on a per pixel basis. MESMA as such permits multiple endmembers for each component and thereby refutes the fixed endmember restriction made in sSMA. In an iterative procedure, based on a spectral library of hundreds of spectra, accounting for each plausible endmember condition, the best-fit model (i.e., lowest RMSE) is assigned to each pixel. Today, this approach is by far the most widely used SMA technique. MESMA has been successfully tested in natural (e.g., Bedini et al., 2009; Eckmann et al., 2008, 2009; Fitzgerald et al., 2005; Li et al., 2005; Okin et al., 2001; Roberts et al., 1998; Sonnetag et al., 2007), urban (e.g., Franke et al., 2009; Powell & Roberts, 2008; Powell et al., 2007; Rashed et al., 2003) and extraterrestrial environments (e.g., Combe et al., 2008; Li & Mustard, 2003) using both multi- (e.g., Peterson & Stow, 2003; Powell et al., 2007; Sonnetag et al., 2007) and hyperspectral optical (e.g., Chabrillat et al., 2000; Chen & Vierling, 2006; Dennison & Roberts, 2003a), and thermal (e.g., Collins et al., 2001; Combe et al., 2008; Eckmann et al., 2009; Foppa et al., 2007) imagery. The capability of MESMA to account for variable endmember conditions is once more demonstrated in Fig. 3. The figure shows the MESMA-based subpixel vegetation cover map derived from the synthetic AISA Eagle image in Fig. 2. Results clearly show an improved resemblance with ground truth, or in other words a significant drop in fraction estimate errors, as compared to sSMA.

In parallel with MESMA, others have introduced alternative mixture cycles. Asner and Lobell (2000) introduced a Monte Carlo spectral unmixing model, AutoMCU. Similar to MESMA a large number of endmember combinations for each pixel are calculated by randomly selecting spectra from a spectral database. AutoMCU is used to propagate uncertainty in endmember spectra to the final subpixel cover fraction results. A minimum, mean and maximum cover fraction image is produced in this so-called fuzzy unmixing technique. The concept of AutoMCU has been subsequently tested in many biomes on the planet and this using a broad variety of airborne and spaceborne sensors (Asner et al., 2003, 2005; Broadbent et al., 2006; Byambakhuu et al., 2010; Gill & Phinn, 2009; Lobell & Asner, 2004; Miao et al., 2006; Roberts et al., 2003b).

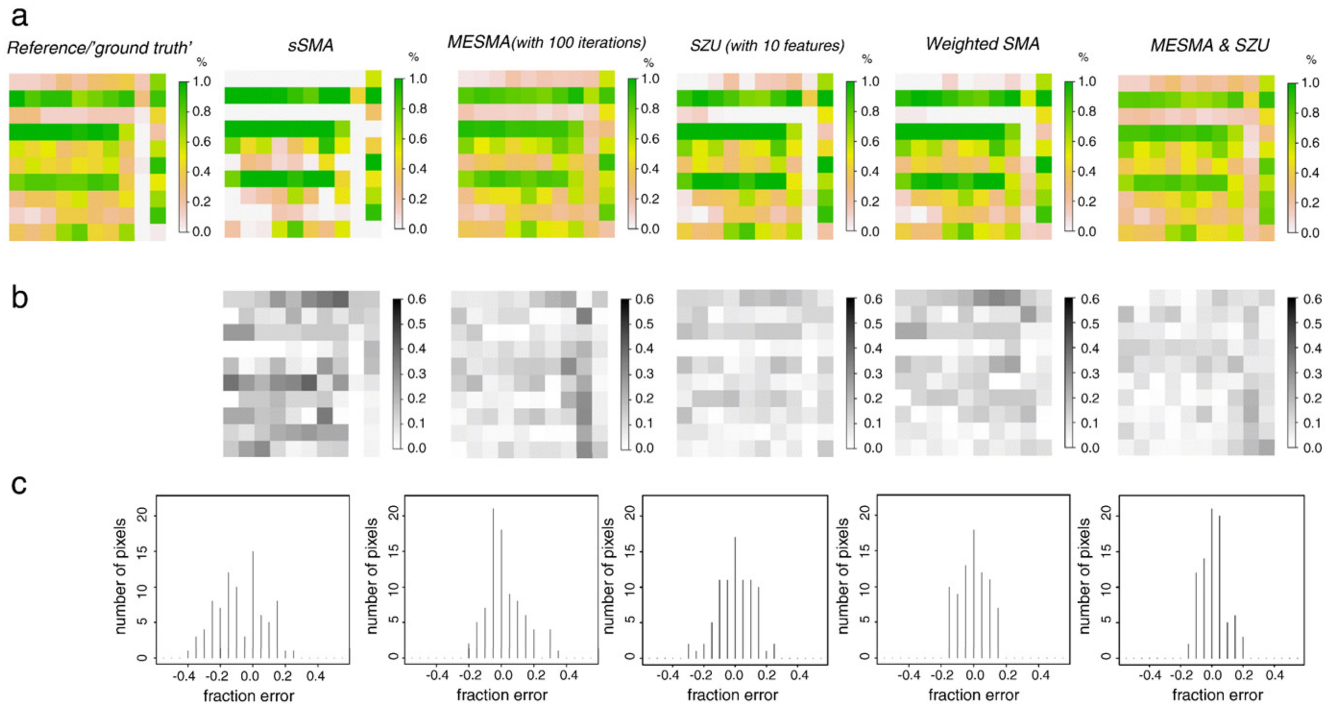

Fig. 3. Subpixel vegetation cover map (a), absolute fraction estimate error map (b) and fraction estimate error histogram (c) for the sSMA, MESMA, SZU and Weighted SMA protocols applied on the AISA Eagle data example introduced in Fig. 2.

An alternative fuzzy unmixing technique was presented by Bateson and Curtiss (1996) and Bateson et al. (2000) as they introduced the concept of endmember bundles to account for the endmember variability in SMA. From the Principal Component Analysis (PCA) eigenvectors of the image data, bundles of vectors are identified to represent the endmembers. A linear programming routine is then used to determine a minimum, mean, and maximum fraction for each endmember. These iterative mixture techniques provide a conceptual framework for understanding the endmember variability and quantifying the introduced uncertainties into fractional estimates.

In the three techniques described, no specific assumption is made concerning the distribution of the endmember population. The probability of a specific endmember to occur was not taken into account in the endmember selection process. To overcome this issue Song (2005) proposed Bayesian Spectral Mixture Analysis (BSMA). The approach works similarly to the other iterative mixture analysis cycles, i.e. each pixel is unmixed with randomly selected combinations of endmember signatures, however, endmember signatures are no longer treated as constants but represented by probability density functions. BSMA as such takes into account the probabilities of spectral signatures, instead of assuming equal probabilities for all endmembers. The approach has been successfully applied to estimate vegetation fractions in the urban environment using both IKONOS and Landsat ETM + images (Song, 2005). A similar approach was tested on AVIRIS images by Dobigeon et al. (2008, 2009).

Iterative unmixing explores a broad variation in endmembers per pixel. Yet, a broad variation in endmembers may lead to more than one possible combination of the pure spectra resulting in the same mixture spectrum (Petrou & Foschi, 1999). A problem commonly referred to as ill posedness. Petrou and Foschi (1999) therefore introduced the Fuzzy Linear Unmixing approach for two-endmember mixtures. For a given set of pure endmember spectra, all possible combinations of endmembers were considered for multiple mixtures. As such, the convex hull of the two pure class clusters is filled with mixture clusters of known proportions. In the same space, the mixed pixels are projected and the number of model samples from each of the possible mixture combinations that are within a predefined distance are counted. These samples are then used to compute the probability and confidences for each mixture combination.

Although iterative mixture analysis cycles have been shown to produce good results, the computational complexity of the method is a major drawback especially when applied on hyperspectral datacubes (Rogge et al., 2006; Somers et al., 2010b). Iterative mixture analysis techniques explore all possible endmember combinations in search for the best (or a set of) solution(s) and the high number of iterations strongly slows down the analysis. In the future, techniques should be developed to optimize the number of necessary iterations in SMA. In this light, ongoing research explores the possibilities of using clustered spectral libraries to speed up iterative mixture analysis.

6.2. Spectral feature selection

In 2000, Asner and Lobell highlighted the potential of data reduction in SMA. The authors stipulated that a careful selection of wavelengths, robust against spectral variability (i.e. minimizing intra- and maximizing inter-class variability), could significantly improve subpixel quantification of fractional material cover, while the problem of computational complexity typical of iterative mixture cycles could be reduced. Preceding studies on the variability of the optical properties of leaf, litter and soil material in semi-arid and arid ecosystems had illustrated that the SWIR2 region from 2050 to 2500 nm is the least dependent on variations in structural and biochemical attributes (Asner, 1998; Asner et al., 2000). This so-called stable spectral zone is therefore selected for use in SMA. An iterative, yet CPU efficient, and automated SWIR2 spectral unmixing algorithm was presented, i.e. AutoSWIR (Asner & Lobell, 2000). The approach was successfully tested in (semi-)arid ecosystems (Asner & Heidebrecht, 2002) and conifer forests (Lobell et al., 2001, 2002). The applicability of AutoSWIR, however, completely depends on the availability of high-fidelity SWIR2 region spectral data and thus depends on sensor performance. In addition, the approach was originally designed for semi-arid and arid environments exploiting the low SWIR2 variability of materials found in these ecosystems. This is not necessarily true for other types of mixtures (e.g., mixtures of different types of vegetation, Somers et al., 2009d, 2010b; vegetation patches in the urban environment, Somers et al., 2010b). In fact, it is more likely that the position, extent and number of stable spectral zones depend on the spatial, spectral and temporal complexity and composition of the endmembers present in the scene. This is why AutoSWIR has not been applied abundantly and was replaced with AutoMCU in 2002. As opposed to AutoSWIR, AutoMCU includes the visible and near-IR (690–740 nm) spectral information.

Later, more generic statistical band selection techniques for SMA were proposed. Selections based on residual analysis (e.g., Ball et al., 2007; Bioucas-Dias & Nascimento, 2008; Miao et al., 2006) and feature extraction approaches based on Principal Component Analysis (PCA; Johnson et al., 1993; Miao et al., 2006) and Discrete Cosine Transform (DCT, Li, 2004) have been explored. These latter techniques have the additional benefit of only incorporating uncorrelated spectral information in SMA. A conventional way to extract PCA- or DCT-based features is to use the first several large-amplitude PCA or DCT coefficients. Experimental results from Li (2004) showed that while these feature extraction methods reduce the dimensionality of spectral data, they did not help to improve abundance estimations. By contrast, Miao et al. (2006) did provide consistent results for the PCA-based SMA and successfully estimated the spatial extent of yellow star thistle infestations using CASI-2 hyperspectral imagery (maximum standard deviation $= \pm 11\%$). These contrasting results highlight the need for a rigorous evaluation of the effectiveness of PCA-based SMA.

A more pragmatic or empirical spectral feature selection technique was presented by Somers et al. (2010b). In the so-called Stable Zone Unmixing (SZU) the wavelength sensitivity towards spectral variability is assessed using the InStability Index (ISI), defined as the ratio of the intra-class (i.e., the sum of the endmember class standard deviations) to the inter-class endmember variability (i.e., average Euclidean distance between the class means). The authors introduced an ISI driven selection protocol to optimize the spectral subset selection by accounting for a tradeoff between the number of wavelengths used in the analysis (i.e., information) and the ISI (i.e., spectral variability). Once endmember bundles are selected, the available wavebands are ordered according to its ISI and the relative change between successive (ordered) wavebands is used to evaluate whether or not the tradeoff criterion is met. As long the criterion is not met, the most unstable wavebands are systematically removed from analysis. The algorithm was tested on a set of scenarios, generated from in situ measured hyperspectral data covering both urban and natural environments under differing conditions. On average an absolute gain in R^2 of the modeled versus the observed subpixel cover fractions of 0.12 compared to AutoSWIR and MESMA were observed while the absolute reduction in fraction abundance error was 0.03. These findings were verified when SZU was applied on the citrus orchard data of Fig. 2. The subpixel vegetation cover estimates, reported in Fig. 3, show a significant increase in accuracy compared to the sSMA outputs but also a slight increase compared to the accuracy of MESMA.

With the increased availability of airborne and in the future spaceborne hyperspectral imagery, the use of spectral feature selection techniques will be a requisite for CPU efficient and effective SMA. Most of the adjacent wavebands in hyperspectral imagery are highly correlated (Delalieux et al., 2007). In techniques such as AutoSWIR and SZU this issue has not been considered. Potential additional gains in CPU efficiency and fraction estimate accuracy could be provided when only de-correlated wavebands are considered in the mixture analysis. Future innovative research efforts should therefore explore the potential benefits of combining e.g. PCA-based unmixing approaches with an ISI driven waveband selection to further reduce endmember variability issues in SMA.

6.3. Spectral weighting

An alternative to reducing the effect of endmember variability in SMA is spectral weighting. Traditionally, all spectral bands are equally weighted in SMA, assuming equally important effects. Weighted Spectral Mixture Analysis (wSMA; Chang & Ji, 2006; Somers et al., 2009d), in contrast, prioritizes spectral bands less sensitive to endmember variability, i.e. by giving them a higher weight in SMA. Experimental results demonstrated that wSMA generally performs better than the traditional unweighted approaches (Chang & Ji, 2006).

Moreover, Somers et al. (2009d) demonstrated a positive correlation between the error variance and the magnitude of the mixed signal for similar levels of endmember variability. This latter causes the spectral features with high reflectance values to contribute more to the SMA solution compared to bands with low or moderate reflected energy. For mixed signals of e.g. vegetation and soils this means that for similar effects of endmember variability over the entire spectrum, the NIR domain, with high reflectance, will dominate model inversion. Stated otherwise, the estimated cover fractions will mainly be influenced or determined by the NIR domain while only marginally by the VIS domain, the latter displaying a lower reflected energy level. This issue is generally overlooked in existing SMA approaches, but can have huge impact on cover fraction estimates. Therefore, Somers et al. (2009d) proposed a two-step weighting operation subsequently addressing (i) the effect of differences in reflected energy among spectral bands and (ii) the effect of endmember variability. Based on the analysis of synthetic mixed pixel spectra compiled of in situ measured spectra of bare soil, citrus tree and weed canopies a mean absolute gain of 0.24 in R^2 and a mean absolute reduction in fraction abundance error of 0.06 could be demonstrated over traditional SMA approaches. Fig. 3 demonstrates the potential of wSMA to reduce residual spectral information caused by endmember variability in a citrus orchard.

6.4. Spectral transformations

Different spectral transformations have been proposed to reduce the effect of endmember variability. Instead of original reflectance data, modified spectral information was used as input of the SMA. Asner and Lobell (2000) introduced a tied spectrum concept to increase endmember separability. The reflectance at one spectral band (the tie point) is subtracted from all other bands. The resulting spectra are referred to as 'tied' to a certain band. In 2004, Wu proposed the Normalized Spectral Mixture Analysis (NSMA) to examine urban composition in Columbus Ohio using Landsat ETM+ data. Endmember spectra were normalized (i.e. divided by its spectral mean) in order to reduce brightness variation. Zhang et al. (2005) applied NSMA to minimize the effect of lichen spectra variability. The authors used a normalized lichen endmember, less sensitive to spatial and temporal variations, to improve its fractional cover estimate. Almost simultaneously, Zhang et al. (2004) presented Derivative Spectral Unmixing (DSU) in which second derivative endmember spectra were used as inputs into SMA to emphasize the inter-class variability, while reducing the intra-class variability. The approach was successfully applied to map the distribution of rock encrusting lichen communities in Jasper, Canada. A similar approach using first derivatives was applied by Debba et al. (2006) to estimate the partial abundance of spectrally similar iron-bearing oxide/hydroxide/sulfate minerals in complex (simulated) mixtures while Somers et al. (2009c) successfully combined both original reflectance spectra and derivative spectra in SMA. Using simulated Airborne Visible Infrared Imaging Spectrometer (AVIRIS) data they succeeded to improve the

Table 1
Overview of the implementation modalities of different endmember variability reduction techniques. Panel (a) lists the spectral transformations needed to be performed on the endmember libraries prior to SMA. Panel (b) highlights the operations needed to be performed on the image data prior to SMA. Panel (c) summarizes the different SMA operations and how the output is presented. Finally, panel (d) indicates possible application caveats for the different techniques.

(a)

	Spectral transformations performed on endmember libraries* prior to SMA		
	*Operation(s) should only be applied once on the endmember library		
Multiple endmember SMA	–	–	–
Monte Carlo unmixing	–	–	–
Endmember bundles	–	–	–
Bayesian SMA	Assessing endmember population distribution		
PCA-based SMA	Principal component analysis	Spectral feature selection	–
Stable Zone unmixing	Instability index (ISI) calculation	ISI based feature selection	–
Derivative Spectral Unmixing	Derivative analysis	(Spectral feature selection)	–
Wavelet-based SMA	Wavelet tranformations	(Spectral feature selection)	–
Weighted SMA	Spectral normalization	ISI calculation	Spectral weighting
Soil Modeling Mixture Analysis	–	–	–
Integrated SMA	Derivative analysis	ISI calculation	ISI based feature selection

(b)

	Spectral transformations performed on image data*prior to SMA	
	*Operation should be applied on each image pixel, i.e. iterative process	
Multiple endmember SMA	–	–
Monte Carlo unmixing	–	–
Endmember bundles	–	–
Bayesian SMA	–	–
PCA-based SMA	Principal component analysis	–
Stable zone unmixing	–	–
Derivative spectral unmixing	Derivative analysis	–
Wavelet-based SMA	Wavelet tranformations	–
Weighted SMA	Spectral normalization	ISI based spectral weighting
Soil Modeling Mixture Analysis	Soil endmember modeling based on reflectance model and SMC inputs	–
AutoSWIR	Tying transformation	–
Integrated SMA	Derivative analysis	–

(c)

	Spectral Mixture Analysis			
	No of spectral features in analysis	Iterative mixture cycles	Endmember selection	*Output*
	(F = full spectral range; S = spectral subset)	*(i.e. multiple SMA cycles per pixel)*	*(R = random; S = standard*; P = based on endmember probility density function)*	*(cover fractions)*
Multiple endmember SMA	F	X	R	from iteration with best model fit
Monte Carlo unmixing	F	X	R	mean output of all iterations
Endmember bundles	F	X	R	mean, maximum and minimum
Bayesian SMA	F	X	P	From iteration with best model fit
PCA-based SMA	S	–	S	output of the single cycle
Stable zone unmixing	S	–	S	output of the single cycle
Derivative spectral unmixing	(S)	–	S	output of the single cycle
Wavelet-based SMA	(S)	–	S	output of the single cycle
Weighted SMA	F	–	S	output of the single cycle
Soil Modeling Mixture Analysis	F	–	S	output of the single cycle
AutoSWIR	S	X	R	mean output of all iterations
Integrated SMA	S	–	S	output of the single cycle

*Commonly standard endmembers are defined as the mean of the endmember libraries

(d)

	Cavaets and remarks
Multiple endmember SMA	Iterative mixture procedure, can be a CPU efficiency burden when applied on hyperspectral data
Monte Carlo unmixing	Iterative mixture procedure, can be a CPU efficiency burden when applied on hyperspectral data
Endmember bundles	Iterative mixture procedure, can be a CPU efficiency burden when applied on hyperspectral data
Bayesian SMA	Iterative mixture procedure, can be a CPU efficiency burden when applied on hyperspectral data
PCA-based SMA	Operational applicability not yet fully explored; literature reports contrasting results
Stable Zone unmixing	Designed for simple environments with a fixed number of limited endmember classes; for complex environments the algorithm should be used in combination with a segmentation approach (e.g., Rogge et al., 2006)
Derivative spectral unmixing	A careful calibration/validation is required as derivatives tend to increase high-frequency noise
Wavelet-based SMA	Operational applicability not yet fully explored
Weighted SMA	Designed for simple environments with a fixed number of limited endmember classes; for complex environments the algorithm should be used in combination with a segmentation approach (e.g., Rogge et al., 2006)

Table 1 (*continued*)

(d)	
	Cavaets and remarks
Soil Modeling Mixture Analysis	Only applicable for mixtures containing a soil endmember; no spectral library needed for the soil endmember but only applicable when a SMC map and an appropriate soil reflectance model are available
AutoSWIR	Only applicable for soil-vegetation mixtures under dry conditions; requires high-fidelity SWIR2 region spectral data
Integrated SMA	A careful calibration/validation is required as derivatives tend to increase high-frequency noise

delineation of weed patches in citrus orchards as compared to the results provided by traditional SMA and DSU approaches.

Derivative analysis tends to increase high frequency noise (Zhang et al., 2004), therefore some researchers have moved into using wavelet analysis, which is demonstrated to be more robust for reduced Signal-to-Noise Ratios (SNR). Li (2004) implemented discrete wavelet transform-based features in SMA. Synthetic mixtures of soybean, large crabgrass and a silt loam soil were analyzed. Theoretical analysis revealed that wavelets increased the separability among endmembers while the abundance estimation deviation was reduced by 30% to 50% compared to the use of original hyperspectral signals or conventional PCA-based features. Rivard et al. (2008) used continuous wavelets instead of original hyperspectral reflectance values and successfully estimated the subpixel abundance fractions of minerals. Despite these promising results, the potential of wavelet-based SMA has not yet been fully explored. The selection of representative endmember spectra from spectral libraries can be more readily defined in the wavelet domain than using original reflectance data such that gains in subpixel fraction estimate accuracy over conventional SMA approaches are anticipated. This is especially true for spectral mixtures of highly similar endmembers such as found in mixed vegetation stands (e.g., van Aardt & Wynne, 2001), mineral mixtures (e.g, van der Meer, 2006) or urban environments (e.g., Wu, 2004). We therefore suggest additional research to focus on implementing wavelet transforms in these complex environments. Furthermore, we believe that the potential of other spectral transformations not yet been implemented in SMA, e.g. continuum removal spectra (Schmidt & Skidmore, 2003), should be investigated further.

6.5. Spectral modeling

The use of radiative transfer models to generate endmember libraries for SMA is a common approach. In 1998, Painter et al. derived snow spectral endmembers of varying grain size from a radiative transfer model specific to a scene's illumination geometry while Peddle et al. (1999) used a reflectance model to create a spectral library of boreal forest canopies. Dennison et al. (2006) and Eckmann et al. (2008) used the MODTRAN radiative transfer model to create a spectral library of emitted radiance endmembers for the subpixel analysis of wildfire properties. In line with these approaches, Somers et al. (2009b) proposed the Soil Modeling Mixture Analysis (SMMA). In an effort to reduce the spectral effects of soil moisture variations, a radiative transfer model for moist soil background (Lobell & Asner, 2002) was implemented in SMA. Instead of using the soil reflectance model to generate an endmember library, spatio-temporal soil moisture content (SMC) data were used to generate the corresponding spectral soil endmember maps used in SMA. Analysis based on simulated mixtures of in situ measured reflectance spectra of citrus canopies and soils under different moisture conditions illustrated that SMMA provides a dynamic and robust technique to account for spatial and temporal variations in soil spectra. Accurate and robust subpixel cover fraction estimates were provided and the accuracy remained consistent over different moisture scenarios ($R^2>0.94$, RMSE<0.03). SMMA is specifically designed to reduce soil moisture effects and will have no value in decomposing mixtures lacking a soil component. Notwithstanding, we are convinced that the concept of assimilating ancillary data through radiative transfer modeling in SMA bears potential to effectively reduce endmember variability problems in general. These assumptions should be validated by future research.

7. Implementation modalities of the endmember reduction techniques

So far the endmember variability issue has mainly been addressed from a producer's perspective. We have assumed that models driven by maximizing model fit are the most useful, especially since endmember selection is necessarily turned over to an algorithm if there are lots of 'flavors' (Adams & Gillespie, 2006) in each endmember bundle. Certainly, accurate cover fraction estimates require that the model fits the data well (except in the case of analysis in which fractions are not constrained to sum to unity; Harsayni & Chang, 1994). However, for most end-users the trade-off between the obtained accuracy and the implementation/application/execution complexity of the approach is a critical consideration. When selecting a methodology for application, an important aspect that end-users always take into account is how feasible it is to quickly apply the methodology, how many input parameters are involved and how difficult it is to set them to obtain appropriate results, how much prior knowledge (if any) is needed in order to run each technique, and what are the main caveats when running the algorithms. Therefore we included a summary Table 1 to provide users with a comprehensive overview of the implementation modalities of different endmember variability reduction techniques.

8. Towards an integrated approach to address endmember variability

The concepts described in Sections 6 and 7 provide a complementary set of rules to reduce the effects of endmember variability in SMA. Most often none or only one of the above mentioned basic principles is implemented to reduce endmember variability, consequently providing only suboptimal solutions. However, Asner and Lobell (2000) combined both iterative unmixing, band selection and transformation in AutoSWIR while Zhang et al. (2004) and Rivard et al. (2008) integrated a band selection technique in respectively DSU and wavelet unmixing. With this review we intend to further stimulate future efforts to merge the different conceptual approaches – iterative mixture analysis cycles, feature selection, weighting operations, spectral transformations, and spectral modeling – to effectively reduce endmember variability problems in SMA. As an illustration, Fig. 3 demonstrates clear improvements in tree cover estimate accuracy for an approach combining the SZU and MESMA protocols. In addition we highlight the need for intercomparison assessments to identify the most robust and most effective techniques for different ecosystems or land use classes and data types. With the exception of MESMA and AutoMCU, most techniques have only been tested for

Table 2
Overview of the validation modalities of techniques to reduce endmember variability in SMA. It is highlighted which of the five basic principles (I: iterative mixture cycle; S: spectral feature selection; W: spectral weighting; T: spectral transformations; M: spectral modeling) are implemented; which data types (sim: simulated imagery; real: real imagery; hyp: hyperspectral optical data; multi: multispectral optical data; thermal: thermal data) and applications are explored (mineral: geological mapping; vegetation: terrestrial ecosystem monitoring; urban: monitoring of urban environments).

	Endmember variability reduction					Data type					Applications		
	I	S	W	T	M	Sim	Real	Hyper	Multi	Thermal	Mineral	Vegetation	Urban
Multiple endmember SMA	X	–	–	–	–	X	X	X	X	X	X	X	X
Monte Carlo unmixing	X	–	–	–	–	–	X	X	X	X	–	X	–
Endmember Bundles	X	–	–	–	–	X	–	X	–	–	–	X	–
Bayesian SMA	X	–	–	–	–	X	X	X	X	–	–	–	X
PCA-based SMA	–	X	–	–	–	X	X	X	–	–	–	X	–
Stable zone unmixing	–	X	–	–	–	X	–	X	–	–	–	X	X
Derivative spectral unmixing	–	(X)	–	X	–	X	–	X	–	–	X	X	X
Wavelet-based SMA	-	(X)	–	X	–	X	X	X	–	–	X	X	X
Weighted SMA	–	–	X	–	–	X	X	X	X	–	–	X	–
Soil modeling mixture Analysis	–	–	–	–	X	X	–	X	–	–	–	X	–
AutoSWIR	X	X	–	X	–	–	X	X	X	–	–	X	–
Integrated SMA	–	X	X	X	–	X	–	X	–	–	–	X	–

a limited set of ecosystems and data types or were only applied on simulated imagery such that the full value of the techniques cannot be evaluated yet. This is evident from Table 2, providing a general overview of the specific validation modalities of different endmember reduction techniques.

Furthermore, the integration of spatial, temporal and spectral information for reducing endmember variability should be promoted. Endmembers can be defined in terms of temporal signatures of reflectance instead of or in addition to spectral signatures (e.g., Dennison & Roberts, 2003b; Lobell & Asner, 2004; Piwowar et al., 1998; Quarmby et al., 1992; Singh & Glenn, 2009). The unmixing of spectrally highly similar objects can as such be improved. For example, the high spectral similarity between different vegetation types often constrains accurate land use classification. When spectral time series are used to define the endmembers, subpixel classification accuracy can drastically increase since plant type specific phenological development cycles will be reflected in different temporal reflectance profiles (Dennison et al., 2007). Similar, the integration of different sources of spectral information can improve subpixel classification. Zhang and Guindon (2009) implemented high-resolution multispectral images from Quickbird to improve the estimation of the subpixel coverage of impervious surfaces and forest canopies within Landsat TM pixels. A similar data integration approach was presented by Zhukov et al. (1999) and Zurita-Milla et al. (2008, 2009). Somers et al. (2009c) proposed to integrate both magnitude (original reflectance) and shape (derivative spectra) related information in a single mixture analysis. Thereby the authors managed to distinguish between the spectral characteristics of weeds and citrus canopies providing improved subpixel cover maps.

In highly variable scenes, such as urban environments, the issue of endmember variability is further aggravated by the spatial heterogeneity in the type and conditions of endmembers. Segmentation approaches, such as those proposed by Van der Meer (1999), Roessner et al. (2001), Theseira et al. (2002), Garcia-Haro et al. (2005), Rogge et al. (2006), Doan and Foody (2007) and Franke et al. (2009) can be used in combination with the techniques described in Section 6 to further reduce endmember variability. The segmentation approaches either use iterative image subsets to identify the endmembers present within each pixel (e.g., Rogge et al., 2006), or, if the intravariability of a certain endmember is too large, create subclasses for both the unmixing and the subsequent classification (Doan & Foody, 2007).

The proper implementation of SMA not only implies addressing the endmember variability problem, but requires a coordinated effort to simultaneously address residual spectral variability caused by nonlinear mixing (Ray & Murray, 1996), bidirectional reflectance effects (Asner et al., 1997), adjacency effects and atmospheric interferences (Settle, 2005). In this light Somers et al. (2009a) made a first step by combining a nonlinear mixing model with MESMA. The Nonlinear MESMA (nMESMA) provided improved subpixel canopy cover estimates when applied on a dataset of in situ measured mixed pixel spectra from citrus orchards compared to the results provided by the traditional sSMA and traditional MESMA approach. nMESMA accounts for both the effects of endmember variability and multiple scattering. Current research efforts are being made towards the development and implementation of submodels accounting for bidirectional reflectance and adjacency effects. These submodels should ultimately be merged with an atmospheric correction algorithm and nMESMA, or an equivalent approach accounting for both endmember variability and multiple scattering events, providing as such an operational technique for subpixel classification.

9. Summary

This review paper focused on the residual spectral information introduced in Spectral Mixture Analysis by the common variability within and among the spectral characteristics of subpixel land cover classes. A state of the art on the available endmember variability reduction techniques is given. Five basic principles are identified: (i) iterative mixture analysis cycles, (ii) spectral feature selection, (iii) spectral weighting operations, (iv) spectral transformations and (v) spectral modeling. The complementarity between the different conceptual approaches is highlighted and it is hypothesized and stressed that the integration of the different concepts is a prerequisite for the effective mitigation of endmember variability in Spectral Mixture Analysis.

Experimental data were used to familiarize readers with the positive effects that endmember variability reduction techniques can have on subpixel fraction estimate accuracy. The results were used as an illustration rather than to provide a comprehensive quantitative intercomparison analysis. To date, experimental results comparing different endmember variability reduction techniques are very scarce. One of the challenges the remote sensing research community is confronted with is to develop an improved experimental understanding of the different unmixing techniques upon which to build an understanding of how to match application and endmember reduction strategies. The current lack of experimental results makes it hard to identify the most robust and most effective technique for a specific ecosystem or data type. With this review we hope to trigger new research initiatives to bridge this knowledge gap.

Acknowledgements

The research presented in this paper is funded by the Belgian Science Policy Office in the frame of the STEREO II programme — project VEGEMIX (SR/67/146). We would like to thank Prof. Gene Albrigo to make available the AISA Eagle image. We are indebted to the editor and referees for their reviews that improved the content of this paper.

References

Adams, J. B., & Gillespie, A. R. (2006). Remote sensing of landscapes with spectral images: A physical modeling approach. Cambridge, UK: Cambridge University Press 362 pp.

Adams, J. B., Sabol, D., Kapos, V., Filho, R. A., Roberts, D. A., Smith, M. O., et al. (1995). Classification of multispectral images based on fractions of endmembers: Application to land-cover change in the Brazilian Amazon. *Remote Sensing of Environment*, *52*, 137—154.

Adams, J. B., Smith, M. O., & Gillespie, A. R. (1993). Imaging spectroscopy: Interpretation based on spectral mixture analysis. In C. M. Pieters & P. Englert (Eds.), *Remote geochemical analysis: Elements and mineralogical composition*. NY: Cambridge Univ. Press 145–166 pp.

Adams, J. B., Smith, M. O., & Johnson, P. E. (1986). Spectral mixture modeling — A new analysis of rock and soil types at the Viking Lander-1 site. *Journal of Geophysical Research, Solid Earth and Planets*, *91*, 8098—8112.

Arai, K. (2007). Nonlinear mixture model of mixed pixels in remote sensing satellite images based on Monte Carlo simulation. *Advances in Space Research*, *41*, 1715—1723.

Asner, G. P. (1998). Biophysical and biochemical sources of variability in canopy reflectance. *Remote Sensing of Environment*, *64*, 234—253.

Asner, G. P., & Heidebrecht, K. B. (2002). Spectral unmixing of vegetation, soil, and dry carbon cover in arid regions: comparing multispectral and hyperspectral observations. *International Journal of Remote Sensing*, *23*, 3939—3958.

Asner, G. P., & Heidebrecht, K. B. (2005). Desertification alters regional ecosystem–climate interactions. *Global Change Biology*, *11*, 182—194.

Asner, G. P., Keller, M., Pereira, R., Zweede, J. C., & Silva, J. N. M. (2003). Scale dependence of biophysical structure in deforested areas bordering the Tapajo's National Forest, Central Amazon. *Remote Sensing of Environment*, *87*, 507—520.

Asner, G. P., Keller, M., Pereira, R., Zweede, J. C., & Silva, J. N. M. (2004). Canopy damage and recovery after selective logging in Amazonia: Field and satellite studies. *Ecological Applications*, *14*, S280—S298.

Asner, G. P., Knapp, D. E., Cooper, A. N., Bustamante, M. M. C., & Olander, L. P. (2005). Ecosystem structure throughout the Brazilian amazon from Landsat observations and automated spectral unmixing. *Earth Interactions*, *9*(7).

Asner, G. P., & Lobell, D. B. (2000). A biogeophysical approach for automated SWIR unmixing of soils and vegetation. *Remote Sensing of Environment*, *74*, 99—112.

Asner, G. P., Wessman, C. A., & Privette, J. L. (1997). Unmixing the directional reflectances of AVHRR subpixel landcovers. *IEEE Transactions on Geoscience and Remote Sensing*, *35*, 868—878.

Asner, G. P., Wessmann, C. A., Bateson, C. A., & Privette, J. L. (2000). Impact of tissue, canopy, and landscape factors on the hyperspectral reflectance variability of arid ecosystems. *Remote Sensing of Environment*, *74*, 69—84.

Atkinson, P. M., Cutler, M. E. J., & Lewis, H. (1997). Mapping sub-pixel proportional land cover with AVHRR imagery. *International Journal of Remote Sensing*, *18*, 917—935.

Atkinson, P. M., & Tatnall, A. R. L. (1997). Neural networks in remote sensing — Introduction. *International Journal of Remote Sensing*, *18*, 699—709.

Ball, J. E., Bruce, L. M., & Younan, N. H. (2007). Hyperspectral pixel unmixing via spectral band selection and DC-insensitive singular value decomposition. *IEEE Geoscience and Remote Sensing Letters*, *4*, 382—386.

Ball, J. E., Kari, S., & Younan, N. H. (2004). Hyperspectral pixel unmixing using singular value decomposition. *Proceedings of the IEEE International Geoscience and Remote Sensing Symposium*, *5*. (pp. 3253—3256).

Barducci, A., & Mecocci, A. (2005). Theoretical and experimental assesment of noise effects on least-squares spectral unmixing of hyperspectral images.*Optical Engineering*, *44* Art. N° 087008.

Bateson, C. A., Asner, G. P., & Wessman, C. A. (2000). Endmember bundles: A new approach to incorporating endmember variability into spectral mixture analysis. *IEEE transactions on geoscience and remote sensing*, *38*, 1083—1094.

Bateson, C. A., & Curtiss, B. (1996). A method for manual endmember selection and spectral unmxiing. *Remote Sensing of Environment*, *55*, 229—243.

Bedini, E. (2009). Mapping lithology of the Sarfartoq carbonatite complex, southern West Greenland, using HyMap imaging spectrometer data. *Remote Sensing of Environment*, *113*, 1208—1219.

Bedini, E., van der Meer, F., & van Ruitenbeek, F. (2009). Use of HyMap imaging spectrometer data to map mineralogy in the Rodalquilar caldera, southeast Spain. *International Journal of Remote Sensing*, *30*, 327—348.

Bioucas-Dias, J. M., & Nascimento, J. M. P. (2008). Hyperspectral subspace identification. *IEEE Transactions on Geoscience and Remote Sensing*, *46*, 2435—2445.

Boardman, J. W., Kruse, F. A., & Green, R. O. (1995). Mapping target signatures via partial unmixing of AVIRIS data. *Summaries, Fifth JPL Airborne Earth Science Workshop. JPL Publication*, *95*. (pp. 23—26).

Borel, C. C., & Gerstl, S. A. (1994). Nonlinear spectral mixing models for vegetative and soil surfaces. *Remote Sensing of Environment*, *47*, 403—416.

Broadbent, E. N., Zarin, D. J., Asner, G. P., Pena-Claros, M., Cooper, A., & Little, R. (2006). Recovery of forest structure and spectral properties after selective logging in lowland Bolivia. *Ecological Applications*, *16*, 1148—1163.

Brown, M., Gunn, S. R., & Lewis, H. G. (1999). Support vector machines for optimal classification and spectral unmixing. *Ecological Modelling*, *120*, 167—179.

Byambakhuu, I., Sugita, M., & Matsushima, D. (2010). Spectral unmixing model to assess land cover fractions in Mongolian steppe regions. *Remote Sensing of Environment*, *114*, 2361—2372.

Carpenter, G. A., Gopal, S., Macomber, S., Martens, S., & Woodstock, C. E. (1999). A neural network method for mixture estimation for vegetation mapping. *Remote Sensing of Environment*, *70*, 138—152.

Chabrillat, S., Pinet, P. C., Ceuleneer, G., Johnson, P. E., & Mustard, J. F. (2000). Ronda peridotite massif: methodology for its geological mapping and lithological discrimination from airborne hyperspectral data. *International Journal of Remote Sensing*, *21*, 2363—2388.

Chang, C. -I., & Heinz, D. C. (2000). Constrained subpixel target detection for remotely sensed imagery. *IEEE Transactions on Geoscience and Remote Sensing*, *38*, 1144—1159.

Chang, C., & Ji, B. (2006). Weighted abundance-constrained linear spectral mixture analysis. *IEEE Transactions on Geoscience and Remote Sensing*, *44*, 378—388.

Chen, J., Jia, X. P., Yang, W., & Matsushita, B. (2009). Generalization of subpixel analysis for hyperspectral data with flexibility in spectral similarity measures. *IEEE Transactions on Geoscience and Remote Sensing*, *47*, 2165—2171.

Chen, X., & Vierling, L. (2006). Spectral mixture analysis of hyperspectral data acquired using a tethered balloon. *Remote Sensing of Environment*, *103*, 338—350.

Collins, E. F., Roberts, D. A., & Borel, C. C. (2001). Spectral mixture analysis of simulated thermal infrared spectrometry data: An initial temperature estimate bounded TESSMA search approach. *IEEE Transactions on Geoscience and Remote Sensing*, *39*, 1435—1446.

Combe, J. P., Le Mouelic, S., Sotin, C., Grendin, A., Mustard, J. F., Le Deit, L., et al. (2008). Analysis of OMEGA/Mars express data hyperspectral data using a Multiple Endmember Linear Spectral Unmixing Model (MELSUM): Methodology and first results. *Planetary and Space Science*, *56*, 951—975.

Craig, M. D. (1994). Minimum-volume transforms for remotely sensed data. *IEEE Transactions on Geoscience and Remote Sensing*, *32*, 542—552.

Debba, P., Carranza, E. J. M., van der Meer, F. D., & Stein, A. (2006). Abundance estimation of spectrally similar minerals by using derivative spectra in simulated annealing. *IEEE Transactions on Geoscience and Remote Sensing*, *44*, 3649—3658.

Delalieux, S., van Aardt, J. A. N., Keulemans, W., Schrevens, E., & Coppin, P. (2007). Detection of biotic stress (Venturia inaequalis) in apple trees using hyperspectral data: non-parametric statistical approaches and physiological implications. *European Journal of Agronomy*, *27*, 130—143.

Dennison, P. E., Charoensiri, K., Roberts, D. A., Peterson, S. H., & Green, R. O. (2006). Wildfire temperature and land cover modeling using hyperspectral data. *Remote Sensing of Environment*, *100*, 212—222.

Dennison, P. E., & Roberts, D. A. (2003a). Endmember selection for multiple endmember spectral mixture analysis using endmember average RMSE. *Remote Sensing of Environment*, *87*, 123—135.

Dennison, P. E., & Roberts, D. A. (2003b). The effects of vegetation phenology on endmember selection and species mapping in Southern California Chaparral. *Remote Sensing of Environment*, *87*, 123—135.

Dennison, P. E., Roberts, D. A., & Peterson, S. H. (2007). Spectral shape-based temporal compositing algorithms for MODIS surface reflectance data. *Remote Sensing of Environment*, *109*, 510—522.

Doan, T. X. H., & Foody, G. M. (2007). Reducing the impacts of intra-class soectral variability on soft classification and its implications for super-resolution mapping. *Geoscience and Remote Sensing Symposium, IGARSS 2007* (pp. 2585—2588).

Dobigeon, N., Moussaoui, S., Coulon, M., Tourneret, J. Y., & Hero, A. O. (2009). Joint Bayesian endmember extraction and linear unmixing for hyperspectral imagery. *IEEE Transactions on Signal Processing*, *57*, 4355—4368.

Dobigeon, N., Tourneret, J. Y., & Chang, C. I. (2008). Semi-supervised linear spectral unmixing using a hierarchical Bayesian model for hyperspectral imagery. *IEEE Transactions on Signal Processing*, *56*, 2684—2695.

Du, Q. (2004). Optimal linear unmixing for hyperspectral image analysis. *Proceedings of the IEEE International Geoscience and Remote Sensing Symposium*, *5*. (pp. 3219—3221).

Eckmann, T. C., Roberts, D. A., & Still, C. J. (2008). Using multiple endmember spectral mixture analysis to retrieve subpixel fire properties from MODIS. *Remote Sensing of Environment*, *112*, 3773—3783.

Eckmann, T. C., Roberts, D. A., & Still, C. J. (2009). Estimating subpixel fire sizes and temperatures from ASTER using multiple endmember spectral mixture analysis. *International Journal of Remote Sensing*, *30*, 5851—5864.

Eckmann, T. C., Still, C. J., Roberts, D. A., & Michaelsen, J. C. (2010). Variations in subpixel fire properties with season and land cover in Southern Africa. *Earth Interactions*, *14*(6).

Elmore, A. J., Mustard, J. F., Manning, S. J., & Lobell, D. B. (2000). Quantifying vegetation change in semiarid environments: Precision and accuracy of spectral mixture analysis and the normalized difference vegetation index. *Remote Sensing of Environment*, *73*, 87—102.

Farrand, W. H., Singer, R. B., & Merenyi, E. (1994). Retrieval of apparent surface reflectance from AVIRIS data — A comparison of empirical line, radiative transfer and spectral mixture methods. *Remote Sensing of Environment*, *47*, 311—321.

Fischer, E. M., & Pieters, C. M. (1994). Remote determination of exposure degree and iron concentration of lunar soils using VIS-NIR spectroscopic methods. *Icarus*, *111*, 475—488.

Fitzgerald, G. J., Pinter, P. J., Hunsaker, D. J., & Clarke, T. R. (2005). Multiple shadow fractions in spectral mixture analysis of a cotton canopy. *Remote Sensing of Environment*, *97*, 526—539.

Foppa, N., Hauser, A., Oesch, D., Wunderle, S., & Meister, R. (2007). Validation of operational AVHRR subpixel snow retrievals over the European Alps based on ASTER data. *International Journal of Remote Sensing*, *28*, 4841−4865.

Franke, J., Roberts, D. A., Halligan, K., & Menz, G. (2009). Hierarchical Multiple Endmember Spectral Mixture Analysis (MESMA) of hyperspectral imagery for urban environments. *Remote Sensing of Environment*, *113*, 1712−1723.

Garcia, M., & Ustin, S. L. (2001). Detection of interannual vegetation responses to climate variability using AVIRIS data in a coastal savanna in California. *IEEE Transactions on Geoscience and Remote Sensing*, *39*, 1480−1490.

Garcia-Haro, F. J., Sommer, S., & Kemper, T. (2005). A new tool for variable multiple endmember spectral mixture analysis (VMESMA). *International Journal of Remote Sensing*, *26*, 2135−2162.

Gilabert, M. A., Garcia-Haro, F. J., & Melia, J. (2000). A mixture modeling approach to estimate vegetation parameters for heterogeneous canopies in remote sensing. *Remote Sensing of Environment*, *72*, 328−345.

Gill, T. K., & Phinn, S. R. (2009). Improvements to ASTER-derived fractional estimates of bare ground in a savanna rangeland. *IEEE Transactions on Geoscience and Remote Sensing*, *47*, 662−670.

Gillespie, A. R. (1992). Spectral mixture analysis of multispectral thermal infrared images. *Remote Sensing of Environment*, *42*, 137−145.

Gong, P., & Zhang, A. (1999). Noise effect on linear spectral unmixing. *Journal of GIS*, *5*, 52−57.

Goodwin, N., Coops, N. C., & Stone, C. (2005). Assessing plantation canopy condition from airborne imagery using spectral mixture analysis and fractional abundances. *International Journal of Applied Earth Observation and Geoinformation*, *7*, 11−28.

Green, R. O., Eastwood, M. L., Sarture, C. M., Chrien, T. G., Aronsson, M., Chippendale, B. J., et al. (1998). Imaging spectroscopy and the Airborne Visible Infrared Imaging Spectrometer (AVIRIS). *Remote Sensing of Environment*, *65*, 227−248.

Guilfoyle, K. J., Althouse, M. L., & Chang, C. -I. (2001). A quantitative and comparative analysis of linear and nonlinear spectral mixture models using radial basis function neural networks. *IEEE Transactions on Geoscience and Remote Sensing*, *39*, 2314−2318.

Harsayni, J. C., & Chang, C. I. (1994). Hyperspectral image classification and dimensionality reduction: an orthogonal subspace projection approach. *IEEE Transactions on Geoscience and Remote Sensing*, *32*, 779−784.

Heinz, D. C., & Chang, C. I. (2001). Fully constrained least squares linear spectral mixture analysis method for material quantification in hyperspectral imagery. *IEEE Transactions on Geoscience and Remote Sensing*, *39*, 529−545.

Hestir, E. L., Khanna, S., Andrew, M. E., Santos, M. J., Viers, J. H., Greenberg, J. A., et al. (2008). Identification of invasive vegetation using hyperspectral remote sensing in the California Delta ecosystem. *Remote Sensing of Environment*, *112*, 4034−4047.

Huang, C. -Y., Asner, G. P., Barger, N. N., Neff, J. C., & Floyd, M. L. (2010). Regional aboveground live carbon losses due to drought-induced tree dieback in pinon-juniper ecosystems. *Remote Sensing of Environment*, *114*, 1471−1479.

Huete, A. R. (1986). Separation of soil-plant spectral mixtures by factor analysis. *Remote Sensing of Environment*, *19*, 237−251.

Jia, G. J., Burke, I. C., Goetz, A. F. H., Kaufmann, M. R., & Kindel, B. C. (2006). Assessing spatial patterns of forest fuel using AVIRIS data. *Remote Sensing of Environment*, *102*, 318−327.

Johnson, P. E., Smith, M. O., Taylorgeorge, S., & Adams, J. B. (1993). A semiempirical method for analysis of the reflectance spectra of binary mineral mixtures. *Journal of Geophysical Research*, *88*, 3557−3561.

Katra, I., & Lancaster, N. (2008). Surface-sediment dynamics in a dust source from spaceborne multispectral thermal infrared data. *Remote Sensing of Environment*, *112*, 3212−3221.

Keshava, N., & Mustard, J. F. (2002). Spectral unmixing. *IEEE Signal Processing*, *19*, 44−57.

Lelong, C. C. D., Pinet, P. C., & Poilvé, H. (1998). Hyperspectral Imaging and Stress Mapping in Agriculture: A Case Study on Wheat in Beauce (France). *Remote Sensing of Environment*, *66*, 179−191.

Li, J. (2004). Wavelet-based feature extraction for improved endmember abundance estimation in linear unmixing of hyperspectral signals. *IEEE Transactions on Geoscience and Remote Sensing*, *42*, 644−649.

Li, L., & Mustard, J. F. (2003). Highland contamination in lunar mare soils: Improved mapping with multiple endmember spectral mixture analysis (MESMA). *Journal of Geophysical Research, Planets*, *108*(5053).

Li, L., Ustin, S. L., & Lay, M. (2005). Application of multiple endmember spectral mixture analysis (MESMA) to AVIRIS imagery for coastal salt marsh mapping: a case study in China Camp, CA, USA. *International Journal of Remote Sensing*, *26*, 5193−5207.

Liu, J. G., Miller, J. R., Haboudane, D., Pattey, E., & Hochhaim, K. (2008). Crop fraction estimation from casi hyperspectral data using linear spectral unmixing and vegetation indices. *Canadian Journal of Remote Sensing*, *34*, S124−S138.

Lobell, D. B., & Asner, G. P. (2002). Moisture effects on soil reflectance. *Soil Science Society of America Journal*, *66*, 722−727.

Lobell, D. B., & Asner, G. P. (2004). Cropland distributions from temporal unmixing of MODIS data. *Remote Sensing of Environment*, *93*, 412−422.

Lobell, D. B., Asner, G. P., Law, B. E., & Treuhaft, R. N. (2001). Subpixel canopy cover estimation of coniferous forests in Oregon using SWIR imaging spectrometry. *Journal of Geophysical Research, [Atmospheres]*, *106*, 5151−5160.

Lobell, D. B., Asner, G. P., Law, B. E., & Treuhaft, R. N. (2002). View angle effects on canopy reflectance and spectral mixture analysis of coniferous forests using AVIRIS. *International Journal of Remote Sensing*, *23*, 2247−2262.

Martinez, P. J., Perez, R. M., Plaza, A., Aguilar, P. L., Cantero, M. C., & Plaza, J. (2006). Endmember extraction algorithms from hyperspectral images. *Annals of Geophysics*, *49*, 93−101.

McGwire, K., Minor, T., & Fenstermaker, L. (2000). Hyperspectral mixture modelling for quantifying sparse vegetation cover in arid environments. *Remote Sensing of Environment*, *72*, 360−374.

Melendez-Pastor, I., Navarro-Pedreno, J., Gomez, I., & Koch, M. (2010). Detecting drought induced environmental changes in a Mediterranean wetland by remote sensing. *Applied Geography*, *30*, 254−262.

Mercier, G., Hubert-Moy, L., Houet, T., & Gouery, P. (2005). Estimation and monitoring of bare soil/vegetation ratio with SPOT VEGETATION and HRVIR. *IEEE Transactions on Geoscience and Remote Sensing*, *43*, 348−354.

Mertes, L. A. K. (2002). Remote Sensing of riverine landscapes. *Freshwater Biology*, *47*, 799−816.

Mertes, L. A. K., Smith, M. O., & Adams, J. B. (1993). Estimating suspended sediment concentrations in surface waters of the Amazon river wetlands from Landsat images. *Remote Sensing of Environment*, *43*, 281−301.

Miao, X., Gong, P., Swope, S., Pu, R., Carruthers, R., Anderson, G. L., et al. (2006). Estimation of yellow starthistle abindance through CASI-2 hyperspectral imagery using linear spectral mixture models. *Remote Sensing of Environment*, *101*, 329−341.

Miao, L., & Qi, H. (2007). Endmember extraction from highly mixed data using minimum volume constrained nonnegative matrix factorization. *IEEE Transactions on Geoscience and Remote Sensing*, *45*, 765−777.

Morton, D. C., DeFries, R. S., Shimabukuro, Y. E., Anderson, L. O., Espirito-Santo, F. D. B., Hansen, M., et al. (2005). Rapid assessment of annual deforestaion in the Brazilian Amazon using MODIS data. *Earth Interactions*, *9*(8).

Mustard, J. F., & Pieters, C. M. (1987). Quantitative abundance estimates from bidirectional reflectance measurements. *Journal of Geophysical Research*, *92*, 617−626.

Mustard, J. F., & Pieters, C. M. (1989). Photometric phase functions of commo geologic minerals and applications to quantitative-analysis of mineral mixture reflectance spectra. *Journal of Geophysical Research*, *10*, 13619−13634.

Nascimento, J. M. P., & Bioucas-Dias, J. M. B. (2005a). Does independent component analysis play a role in unmixing hyperspectral data? *IEEE Transactions on Geoscience and Remote Sensing*, *43*, 175−187.

Nascimento, J. M. P., & Bioucas-Dias, J. M. B. (2005b). Vertex component analysis: a fast algorithm to unmix hyperspectral data. *IEEE Transactions on Geoscience and Remote Sensing*, *43*, 898−910.

Nash, D. B., & Conel, J. E. (1974). Spectral reflectance systematics for mixtures of powdered hypersthene, labradorite, and ilmenite. *Journal of Geophysical Research*, *79*, 1615−1621.

Okin, G. S., Roberts, D. A., Murray, B., & Okin, W. J. (2001). Practical limits on hyperspectral vegetation discrimination in arid and semiarid environments. *Remote Sensing of Environment*, *77*, 212−225.

Pacheco, A., & McNairn, H. (2010). Evaluating multispectral remote sensing and spectral unmixing analysis for crop residue mapping. *Remote Sensing of Environment*, *114*, 2219−2228.

Painter, T. H., Dozier, J., Roberts, D. A., Davis, R. E., & Green, R. O. (2003). Retrieval of subpixel snow-covered area and grain size from imaging spectrometer data. *Remote Sensing of Environment*, *85*, 64−77.

Painter, T. H., Roberts, D. A., Green, R. O., & Dozier, J. (1998). The effect of grain size on spectral mixture analysis of snow covered area from AVIRIS data. *Remote Sensing of Environment*, *65*, 320−332.

Peddle, D. R., Hall, F. G., & LeDrew, E. F. (1999). Spectral mixture analysis and geometric-optical reflectance modeling of boreal forest biophysical structure. *Remote Sensing of Environment*, *67*, 288−297.

Peddle, D. R., & Smith, M. (2005). Spectral mixture analysis of agricultural crops: endmember validation and biophysical estimation in potato plots. *International Journal of Remote Sensing*, *26*, 4959−4979.

Peterson, S. H., & Stow, D. A. (2003). Using multiple image endmember spectral mixture analysis to study chaparral regrowth in southern California. *International Journal of Remote Sensing*, *24*, 4481−4504.

Petrou, M., & Foschi, P. G. (1999). Confidence in linear spectral unmixing of single pixels. *IEEE Transactions on Geoscience and Remote Sensing*, *37*, 624−626.

Phinn, S., Stanford, M., Scarth, P., Murray, A. T., & Shyy, P. T. (2002). Monitoring the composition of urban environments based on the vegetation-impervious surface-soil (VIS) model by subpixel analysis techniques. *International Journal of Remote Sensing*, *23*, 4131−4153.

Pinet, P. C. (1995). Spectroscopic imaging of solid planetary surfaces. *Tridimensional optical spectroscopic methods in Astrophysics*, *71*. (pp. 294−297).

Piwowar, J. M., Peddle, D. R., & LeDrew, E. F. (1998). Temporal mixture analysis of Arctic Sea ice imagery: a new approach for monitoring environmental change. *Remote Sensing of Environment*, *63*, 195−207.

Plaza, A., Martinez, P., Perez, R., & Plaza, J. (2002). Spatial/spectral endmember extraction by multidimensional morphological operations. *IEEE Transactions on Geoscience and Remote Sensing*, *40*, 2025−2041.

Plaza, A., Martinez, P., Perez, R., & Plaza, J. (2004). A quantitative and comparative analysis of endmember extraction algorithms from hyperspectral data. *IEEE Transactions on Geoscience and Remote Sensing*, *42*, 650−663.

Plaza, A., Martinez, P., Plaza, J., & Perez, R. (2005). Dimensionality reduction and classification of hyperspectral image data using sequences of extended morphological transformations. *IEEE Transactions on Geoscience and Remote Sensing*, *43*, 466−479.

Powell, R. L., & Roberts, D. A. (2008). Characterizing variability of the urban physical environment for a suite of cities in Rondonia, Brazil. *Earth Interactions*, *12*(13).

Powell, R. L., Roberts, D. A., Dennison, P. E., & Hess, L. L. (2007). Sub-pixel mapping of urban land cover using multiple endmember spectral mixture analysis: Manaus, Brazil. *Remote Sensing of Environment*, *106*, 253−267.

Quarmby, N. A., Townshend, J. R. G., Settle, J. J., White, K. H., Milnes, M., Hindle, T. L., et al. (1992). Linear mixture modeling applied to AVHRR data for crop area estimation. *International Journal of Remote Sensing*, *13*, 415−425.

Radeloff, V. C., Mladenoff, D. J., & Boyce, M. S. (1999). Detecting Jack Pine budworm defoliation using spectral mixture analysis: Separating effects from determinants. *Remote Sensing of Environment*, *69*, 156−169.

Ramsey, M. S., & Christensen, P. R. (1998). Mineral abundance determination: quantitative deconvolution of thermal emission spectra. *Journal of Geophysical Research, Solid Earth*, *103*, 577−596.

Rashed, T., Weeks, J. R., Roberts, D. A., Rogan, J., & Powell, R. (2003). Measuring the physical composition of urban morphology using multiple endmember spectral mixture models. *Photogrammetric Engineering and Remote Sensing*, *69*, 1011−1020.

Ray, T. W., & Murray, B. C. (1996). Nonlinear Spectral Mixing in Desert Vegetation. *Remote Sensing of Environment*, *55*, 59−64.

Rivard, B., Feng, J., Gallie, A., & Sanchez-Azofeifa, A. (2008). Continuous wavelets for the improved use of spectral libraries and hyperspectral data. *Remote Sensing of Environment*, *112*, 2850−2862.

Roberts, D. A. (1991). *Separating spectral mixtures of vegetation and soil*. University of Washington PhD. Dissertation, 180 pp.

Roberts, D. A., Dennison, P. E., Gardner, M. E., Hetzel, Y., Ustin, S. L., & Lee, C. T. (2003a). Evaluation of the potential of Hyperion for fire danger assessment by comparison to the Airborne Visible/Infrared Imaging Spectrometer. *IEEE Transactions on Geoscience and Remote Sensing*, *41*, 1297−1310.

Roberts, D. A., Gardner, M., Church, R., Ustin, S., Scheer, G., & Green, R. O. (1998). Mapping Chaparral in the Santa Monica Mountains Using Multiple Endmember Spectral Mixture Models. *Remote Sensing of Environment*, *65*, 267−279.

Roberts, D. A., Keller, M., & Soares, J. V. (2003b). Studies of land-cover, land-use, and biophysical properties of vegetation in the Large Scale Biosphere Atmosphere experiment in Amazonia. *Remote Sensing of Environment*, *87*, 377−388.

Roberts, D. A., Smith, M. O., & Adams, J. B. (1993). Green vegetation, nonphotosynthetic vegetation, and soils in AVIRIS data. *Remote Sensing of Environment*, *44*, 255−269.

Roberts, D. A., Smith, M. O., Sabol, D. E., Adams, J. B., & Ustin, S. (1992). Mapping the Spectral Variability in Photosynthetic and Non-Photosynthetic Vegetation, Soils and Shade using AVIRIS. *Summaries 3rd Annual JPL Airborne Geoscience Workshop: Vol. 1, AVIRIS, Pasadena, CA. June 1 and 2, 1992* 38–40 pp.

Roberts, D. A., Ustin, S. L., Ogunjemiyo, S., Greenberg, J., Dobrowski, S. Z., Chen, J. Q., et al. (2004). Spectral and structural measures of northwest forest vegetation at leaf to landscape scales. *Ecosystems*, *7*, 545−562.

Roder, A., Udelhoven, T., Hill, J., del Barrio, G., & Tsiourlis, G. (2008). Trend analysis of Landsat-TM and –ETM+ imagery to monitor grazing impact in a rangeland ecosystem in Norther Greece. *Remote Sensing of Environment*, *112*, 2863−2875.

Roessner, S., Segl, K., Heiden, U., & Kaufman, H. (2001). Automated differentiation of urban surfaces base don airborne hyperspectral imagery. *IEEE Transactions on Geoscience and Remote Sensing*, *39*, 1525−1532.

Rogan, J., Franklin, J., & Roberts, D. A. (2002). A comparison of methods for monitoring multitemporal vegetation change using Thematic Mapper imagery. *Remote Sensing of Environment*, *80*, 143−156.

Rogge, D. M., Rivard, B., Zhang, J., & Feng, J. (2006). Iterative spectral unmixing for optimizing per-pixel endmember sets. *IEEE Transactions on Geoscience and Remote Sensing*, *44*, 3725−3736.

Sabol, D. E., Adams, J. B., & Smith, M. O. (1992). Quantitative subpixel spectral detection of targets in multispectral images. *Journal of Geophysical Research, Planets*, *97*, 2659−2672.

Schmidt, K. S., & Skidmore, A. K. (2003). Spectral discrimination of vegetation types in a coastal wetland. *Remote Sensing of Environment*, *85*, 92−108.

Settle, J. (2005). On the residual term in the linear mixture model and its dependence on the point spread function. *IEEE Transactions on Geoscience and Remote Sensing*, *43*, 398−401.

Settle, J. (2006). On the effect of variable endmember spectra in the linear mixture model. *IEEE Transactions on Geoscience and Remote Sensing*, *44*, 389−396.

Shipman, H., & Adams, J. B. (1987). Detectability of minerals in desert alluvial fans using reflectance spectra. *Journal of Geophysical Research*, *92*, 10391−10492.

Singh, N., & Glenn, N. F. (2009). Multitemporal spectral analysis for cheatgrass (Bromus tectorum) classification. *International Journal of Remote Sensing*, *30*, 3441−3462.

Small, C. (2001). Estimation of urban vegetation abundance by spectral mixture analysis. *International Journal of Remote Sensing*, *22*, 1305−1334.

Smith, M. O., Adams, J. B., & Sabol, D. E. (1994). Spectral mixture analysis - new strategies for the analysis of multispectral data. In J. Hill & J. Megier (Eds.), *Imaging Spectrometry - a Tool for Environmental Observations, ECSC, EEC* (pp. 125−143). Brussels and Luxembourg: EAEC.

Smith, M. O., Ustin, S. L., Adams, J. B., & Gillespie, A. R. (1990). Vegetation in Deserts: I. A regional measure of abundance from multispectral images. *Remote Sensing of Environment*, *31*, 1−26.

Soenen, S. A., Peddle, D. R., Hall, R. J., Coburn, C. A., & Hall, F. G. (2010). Estimating aboveground forest biomass from canopy reflectance model inversion in mountainous terrain. *Remote Sensing of Environment*, *114*(7), 1325−1337.

Somers, B., Cools, K., Delalieux, S., Stuckens, J., Van der Zande, D., Verstraeten, W. W., et al. (2009a). Nonlinear Hyperspectral Mixture Analysis for tree cover estimates in orchards. *Remote Sensing of Environment*, *113*, 1183−1193.

Somers, B., Delalieux, S., Stuckens, J., Verstraeten, W. W., & Coppin, P. (2009b). A weighted Linear Spectral Mixture Analysis approach to address endmember variability in agricultural production systems. *International Journal of Remote Sensing*, *30*, 139−147.

Somers, B., Delalieux, S., Verstraeten, W. W., & Coppin, P. (2009c). A conceptual framework for the simultaneous extraction of sub-pixel spatial extent and spectral characteristics of crops. *Photogrammetric Engineering and Remote Sensing*, *75*, 57−68.

Somers, B., Delalieux, S., Verstraeten, W. W., van Aardt, J. A. N., Albrigo, G., & Coppin, P. (2010a). An automated waveband selection technique for optimized hyperspectral mixture analysis. *International Journal of Remote Sensing*, *31*, 5549−5568.

Somers, B., Delalieux, S., Verstraeten, W. W., Verbesselt, J., Lhermitte, S., & Coppin, P. (2009d). Magnitude and shape related feature integration in hyperspectral mixture analysis to monitor weeds in citrus orchards. *IEEE Transactions on Geoscience and Remote Sensing*, *47*, 3630−3642.

Somers, B., Verbesselt, J., Ampe, E. M., Sims, N., Verstraeten, W. W., & Coppin, P. (2010b). Spectral mixture analysis to monitor defoliation in mixed aged Eucalyptus globules Labill plantations in southern Australia using Landsat 5TM and EO-1 Hyperion data. *International Journal of Applied Earth Observation and Geoinformation*, *12*, 270−277.

Song, C. H. (2005). Spectral mixture analysis for subpixel vegetation fractions in the urban environment: How to incorporate endmember variability? *Remote Sensing of Environment*, *95*, 248−263.

Sonnetag, O., Chen, J. M., Roberts, D. A., Talbot, J., Halligan, K. Q., & Govind, A. (2007). Mapping tree and shrub leaf area indices in an ombrotrophic peatland through multiple endmember spectral unmixing. *Remote Sensing of Environment*, *109*, 342−360.

Sunshine, J. M., & Pieters, C. M. (1993). Estimating modal abundances from the spectra of natural and laboratory pyroxene mixtures using the modified Gaussian model. *Journal of Geophysical Research, Planets*, *98*, 9075−9987.

Svab, E., Tyler, A. N., Preston, T., Presing, M., & Balogh, K. V. (2005). Characterizing the spectral reflectance of algae in lake waters with high suspended sediment concentrations. *International Journal of Remote Sensing*, *26*, 919−928.

Theseira, M. A., Thomas, G., & Sannier, C. A. D. (2002). An evaluation of spectral mixture modeling applied to a semi-arid environment. *International Journal of Remote Sensing*, *23*, 687−700.

Theseira, M. A., Thomas, G., Taylor, J. C., Gemmell, F., & Varjo, J. (2003). Sensitivity of mixture modeling to endmember selection. *International Journal of Remote Sensing*, *24*, 1559−1575.

Tompkins, S., Mustard, J. F., Pieters, C. M., & Forsyth, D. W. (1997). Optimization of endmembers for spectral mixture analysis. *Remote Sensing of Environment*, *59*, 472−489.

Tu, T. M., Chen, C. H., & Chang, C. -I. (1997). A posteriori least squares orthogonal subspace projection approach to desired signature extraction and detection. *IEEE Transactions on Geoscience and Remote Sensing*, *35*, 127−139.

van Aardt, J. A. N., & Wynne, R. H. (2001). Spectral separability among six southern tree species. *Photogrammetric Engineering and Remote Sensing*, *67*, 1367−1375.

Van der Meer, F. (1999). Iterative spectral unmixing (ISU). *International Journal of Remote Sensing*, *20*, 3431−3436.

Van der Meer, F. (2006). The effectiveness of spectral similarity measures for the analysis of hyperspectral imagery. *International Journal of Applied Earth Observation and Geoinformation*, *8*, 3−17.

Veganzones, M. A., & Grana, M. (2008). Endmember extraction methods: a short review. *Knowledge-Based Intelligent Information and Engineering Systems, 12th International Conference, KES 2008* (pp. 400−407).

Wang, F. (1990). Fuzzy supervised classification of remote sensing images. *IEEE Transactions on Geoscience and Remote Sensing*, *28*, 194−201.

Wang, J., & Chang, C. -I. (2006). Application of independent component analysis in endmember extraction and abundance quantification for hyperspectral imagery. *IEEE Transactions on Geoscience and Remote Sensing*, *44*, 2601−2616.

Weng, Q., & Hu, X. (2008). Medium spatial resolutionsatellite imagery for estimating and mapping urban impervious surfaces using LSMA and ANN. *IEEE Transactions on Geoscience and Remote Sensing*, *46*, 2397−2406.

Weng, Q. H., Lu, D. S., & Schubring, J. (2004). Estimation of land surface temperature-vegetation abundance relationship for urban heat island studies. *Remote Sensing of Environment*, *89*, 467−483.

Wessman, C. A., Bateson, C. A., & Benning, T. L. (1997). Detecting fire and grazing patterns in tallgrass prairie using spectral mixture analysis. *Ecological Applications*, *7*, 493−511.

Winter, M. E. (1999). N-FINDER: an algorithm for fast autonomous spectral endmember determination in hyperspectral data. *Proceedings of SPIE*, *3753*, 266−275.

Wu, C. (2004). Normalized spectral mixture analysis for monitoring urban composition using ETM^{+} imagery. *Remote Sensing of Environment*, *93*, 480−492.

Wu, C. S., & Murray, A. T. (2003). Estimating impervious surface distribution by spectral mixture analysis. *Remote Sensing of Environment*, *84*, 493−505.

Xu, S. Y., Peddle, D. R., Coburn, C. A., & Kienzle, S. (2008). Sensitivity of a carbon and productivity model to climate, water, terrain, and biophysical parameters in a Rocky Mountain watershed. *Canadian Journal of Remote Sensing*, *34*, 245−258.

Zarco-Tejada, P. J., Miller, J. R., Noland, T. L., Mohammed, G. H., & Sampson, P. H. (2001). Scaling-up and model inversion methods with narrow-band optical indices for chlorophyll content estimation in closed forest canopies with hyperspectral data. *IEEE Transactions on Geoscience and Remote Sensing*, *39*, 1491−1507.

Zhang, Y., & Guindon, B. (2009). Multi-resolution integration of land cover for sub-pixel estimation of urban impervious surface and forest cover. *International Journal of Digital Earth*, *2*, 89−108.

Zhang, J., Rivard, B., & Sanchez-Azofeifa, A. (2004). Derivative spectral unmixing of hyperspectral data applied to mixtures of lichen and rock. *IEEE Transactions on Geoscience and Remote Sensing*, *42*, 1934−1940.

Zhang, J., Rivard, B., & Sanchez-Azofeifa, A. (2005). Spectral unmixing of normalized reflectance data for the deconvolution of lichen and rock mixtures. *Remote Sensing of Environment*, *95*, 57−66.

Zhang, J., Rivard, B., Sanchez-Azofeifa, A., & Castro-Esau, K. (2006). Intra- and inter-class spectral variability of tropical tree species at La Selva, Costa Rica: Implications for species identification using HYDICE imagery. *Remote Sensing of Environment*, *105*, 129−141.

Zhao, X. F., & Qiu, Q. Y. (2009). Spectrtal mixture analysis of land surface composition in a coastal city based on the V-I-S mode. *Joint Urban Remote Sensing Events*, *1*, 1489−1494.

Zhukov, B., Oertel, D., Lanzl, F., & Reinhackel, G. (1999). Unmixing-based multisensor multiresolution image fusion. *IEEE Transactions on Geoscience and Remote Sensing*, *37*, 1212−1226.

Zurita-Milla, R., Clevers, J. G. P. W., & Schaepman, M. E. (2008). Unmixing-based Landsat TM and MERIS FR data fusion. *IEEE Geoscience and Remote Sensing Letters*, *5*, 453−457.

Zurita-Milla, R., Kaiser, G., Clevers, J. G. P. W., Schneider, W., & Schaepman, M. E. (2009). Downscaling time series of MERIS full resolution data to monitor vegetation seasonal dynamics. *Remote Sensing of Environment*, *113*, 1874−1885.